J. Cosmet. Sci., 52, 91–102 (March/April 2001)

Skin optics revisited by *in vivo* confocal microscopy: Melanin and sun exposure

PIERRE CORCUFF, CÉLINE CHAUSSEPIED,
GENEVIÈVE MADRY, and CHRISTOPHE HADJUR, *L'Oréal*
Recherche, Laboratoires de Recherche Avancée,
93601 Aulnay-sous-bois, France.

Accepted for publication February 28, 2001. Presented at the XXIth International IFSCC Congress, Berlin, 2000.

Synopsis

A new confocal prototype dedicated to the exploration of *in vivo* human skin has been constructed around a laser confocal module (Oz Noran, Inc.) and a skin contact device, assuring perfect stability of skin images. The power of the Argon/Krypton laser source has been limited to 2mW to secure safety, and the laser provides three visible wavelengths: 488, 568, and 647 nm. Optical sections were digitized at video rate, providing easy and rapid measurements of the thickness of epidermal layers and time-resolved information. Unexpected details of the epidermis were recorded with the blue laser line. Melanin provided strong reflection of the basal keratinocytes instead of the absorption expected. The 3D reconstruction of the melanin cap in basal keratinocytes confirmed the behavior of melanosomes acting as myriads of nanomirrors that reflected light. Confocal images of the posterior aspect of the forearm were recorded before sun exposure and then for one month after exposure. There was a 25% increase in the thickness of the stratum corneum. Bright inclusions into the dark nucleus of numerous spinous cells were interpreted as local condensation of chromatin. Numerous bright intercellular filaments were attributed to melanosomes filling up dendrites of melanocytes. A striking observation concerned the lack of melanosome caps in basal keratinocytes. *In vivo* confocal microscopy affords new insight to the role of melanin and its gradual migration after sun exposure.

INTRODUCTION

The way by which light penetrates through skin tissue remains a complex phenomenon due to the multiple stratification layers as well as the biochemical composition of the epidermal and dermal layers. It has been established that skin optics respects the rules of absorption, reflection, and scattering (1–3). Absorption coefficients have been experimentally determined and mainly depend upon the content of melanin in the epidermis and the blood perfusion (hemoglobin) in the dermis. They rapidly decrease at longer wavelengths. Reflection corresponds to the index mismatch at various interfaces, i.e., air/skin surface, water/protein, etc. (4). Reduced scattering involves the heterogeneous organization of the dermis and the anisotropy of the collagen network. It follows the Raleigh limit, exhibiting the well-known λ^{-4} behavior (5). In such a context, *in vivo*

confocal microscopy uses a reflected signal to form an image whose contrast is improved by strong reflection and by a limited lack of photons due to absorption and scattering.

Moreover, confocal microscopy of the skin requires real-time imaging to limit blurring caused by motion, i.e., blood flow pulses and involuntary movement. Until recently, the tandem scanning microscope (TSM) was the only technique having this prerequisite of real-time imaging, since confocal laser scanners (CLSM) would typically need a few seconds to form an image. In 1991, the first *in vivo* images at the surface and below the surface of the skin were obtained by using a TSM-based ophthalmoscope (6). From this first attempt, a commercial TSM was redesigned in 1993 (7) for *in vivo* skin imaging with the development of a skin-contact stabilization device fitted around an objective lens that flattened the skin and limited image shifts. The Anderson team (8) solved the slow scan drawback of the CLSM in 1995 by introducing a rotating polygon mirror in the scanning path that produced video-rate images of the human skin *in vivo*.

We describe in this report the design of a new video-rate CLSM prototype adapted to the *in vivo* exploration of human skin that produces sharper reflected-light images. It has been used to depict the various epidermal layers. An explanation of the strong reflection of the basal keratinocytes is proposed. The influence of sun exposure on cellular damage and on melanin migration was likewise investigated.

MATERIALS AND METHODS

THE *IN VIVO* CLSM PROTOTYPE

The prototype was constructed around the compact Oz fast-scanning confocal module manufactured by Noran Instruments Inc. and with the contact-stabilization device designed in-house. A Nikon ×40, 1.30 N.A., oil-immersion objective lens of 160-mm tube length was screwed into a microscope tube directly attached to the scanning-light exit of the confocal module. The rapid Z direction scan (up to 30 optical sections per second) was performed by moving the objective lens with a piezoelectric driver having a maximum travel of 350 μm. The contact device was centered in front of the objective lens. The distance between the lens and the contact tip can be adjusted with coarse and fine manual screws (Figure 1). In this configuration, it is the objective lens that moves vertically while the skin surface remains fixed.

The confocal scanner has a two-channel configuration that permits simultaneous imaging of reflected (scattered) light and fluorescence contrast. A galvanometer-mounted mirror was used to scan the slow axis while an acousto-optic deflector (AOD) was used to scan the fast axis. The latter was a solid-state device that provided variable scanning rates ranging from several seconds per image up to 30 images per second and higher. It was designed to deliver 1000 resolved points within its operating range. The confocal head was suspended from a cantilever arm that gave access to the skin surface of the whole human body (9). Easy positioning of the scanning head was provided by a motorized stage. The light source consisted of a Krypton/Argon laser with power limited to 2 mW at the objective lens in order to avoid photodamage to the skin tissue. The laser provided three wavelengths: 488, 568, and 647 nm. A Silicon Graphics workstation was used to control the system and also performed the capture of a digital image stream generated by the control electronics. The acquisition time was limited only by the

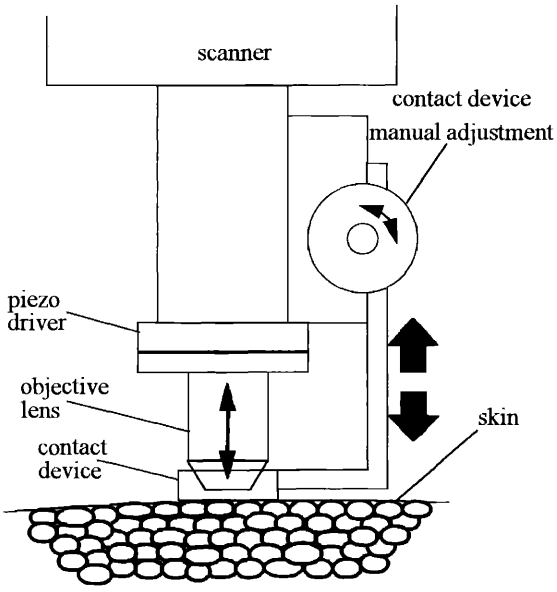

Figure 1. Schema of the *in vivo* confocal module. Rapid Z-scan piezo objective driver and contact device.

availability of memory space (RAM) in the workstation, but was typically about ten seconds for standard size images (512 × 480 pixels) at video-image rates. The control electronics regulated the position of the piezo driver through the piezo control by synchronizing the driver with the timing of the video stream. Thus, the acquisition of depth series (Z-series) or time series (t-series) was done at intervals fast enough to avoid severe shifts between the optical sections. The resulting image stack (data sections) could then be processed in a few minutes for volume rendering and thickness measurements of the various epidermal layers (10).

Z-series formed of 80 optical sections separated by 1-μm steps were acquired on the forearm. The stacks were processed with the OTIP3D software (LISA Labs, CPE, Lyon, France), using first the wavelets algorithm (11) for noise reduction and then the region-growing algorithm (12) for the binarization of convex features. The 3D reconstruction could easily be examined from any view angle with the volume-rotating capability of the software.

SUN EXPOSURE EXPERIMENT

Two volunteers spent one week on a Caribbean beach, free of any experimental constraints. Subject A was a 32-year-old male, having skin phototype III according to the classification of Fitzpatrick (13). Subject B was a 30-year-old female, having skin phototype III. *In vivo* confocal images of the dorsal forearm of each subject were recorded using the blue laser line before exposure (T0), two days after the ten-day trip (T12), ten days (T20) and 30 days (T40). The stratum corneum thickness was automatically measured by using the OTIP3D software from six stacks of optical sections per time-set.

RESULTS

REFLECTION IMAGES OF THE EPIDERMIS

Keratinocytes of the spinous layers of the epidermis were identified by their dark nuclei

(Figure 2a). The cytoplasm exhibited varying bright features corresponding to cytoplasm organelles and/or melanin granules. The plasma membrane was clearly defined. Near the dermo-epidermal junction, a monolayer of bright basal cells (Figure 2b) surrounded the dermal papillae in clusters arranged in the shape of bouquets at the top. At deeper levels these clusters appeared as crowns. In the center of the dermal papillae, dark rounded areas (not shown) indicated the presence of capillary loops where the flow of red blood cells and leukocytes could be watched in movement as a series of time frames.

The 3D reconstruction of a volume of living skin permitted an observation of the relationships between the various segmented features: the keratinocytes identified by their nuclei (Figure 3a), the stratum corneum as an overlay (Figure 3b), and the dermal tissue on the ground. This mode of representation demonstrates that thickness measurements can be automatically extracted from the whole field of exploration, thus ensuring good accuracy of the results.

The 3D reconstruction of the bright features in the basal cells layering a dermal papilla is shown in Figure 4a. By zooming and rotating one of the segmented features (Figure 4b), its lower side clearly revealed a non-convex hull that could be easily associated with the imprint of the nucleus. Thus, the shape and size of this non-convex volume could be attributed to the melanin cap covering the apical pole of the nucleus.

SUN EXPOSURE

The evolution of the stratum corneum thickness followed the same pattern for the two subjects even though individual variations could be recorded (Figure 5). There was a 25% increase at T12 for each subject, which was confirmed at T20. A decrease at T40 was more pronounced for subject B, which recovered almost its initial value.

Unusual histologic changes occurred within the whole epidermis after exposure. First, bright inclusions inside numerous nuclei of granular and spinous keratinocytes (Figure

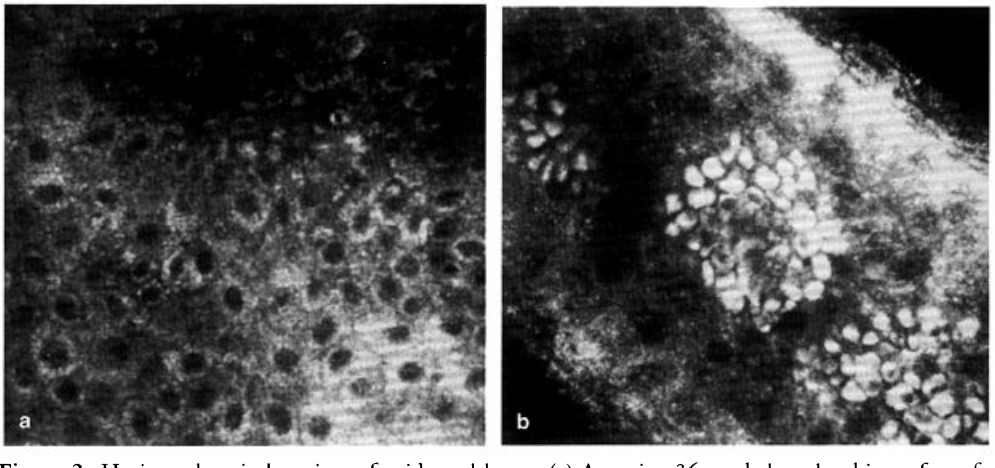

Figure 2. Horizontal optical sections of epidermal layers. (a) A section 36 µm below the skin surface of a Caucasian skin sample. Each keratinocyte contains a dark nucleus, bright features, in the cytoplasm enclosed in the plasma membrane; 488-nm blue laser line. Image size: 180 × 168 µm. (b) A section 48 µm below the skin surface of a Negroid skin sample showing three dermal papillae delineated with bright basal cells forming bouquets and crown; 488-nm blue laser line. Image size: 180 × 168 µm.

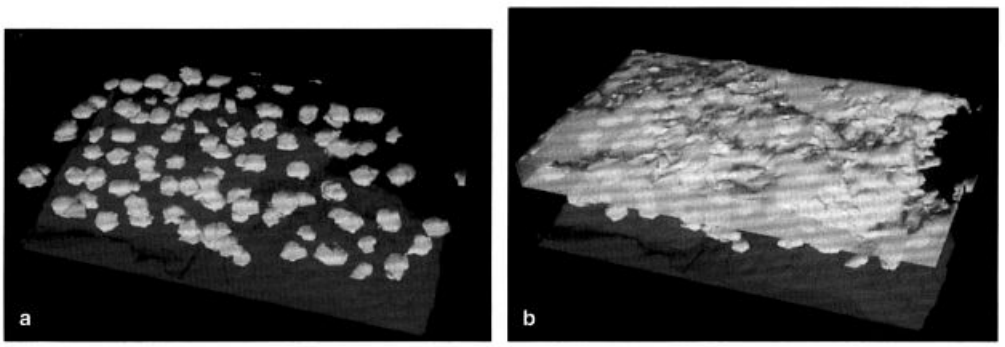

Figure 3. 3D reconstruction of the epidermis from a stack of 66 optical sections, 1-μm steps. The segmented features correspond to: (a) The dermo-epidermal junction in grey tone and the nuclei of spinous and granular keratinocytes in white. The basal epidermal layer is not represented. (b) The stratum corneum represented as a semitransparent light-grey overlay.

6a) persisted up to T20 while almost disappearing at T40. The zoomed image (Figure 6b) clearly shows the shape and size of four inclusions within a dark nucleus. Second, brightly spotted filaments running between keratinocytes were observed at T12 and T20. They had a preferential vertical orientation within the epidermis and seemed to follow the intercellular route (Figures 7a and 7b). Third, melanin caps observed at T0 (Figure 8a) were no longer detected at the site of the usual bright basal monolayer (Figure 8b). This lack of melanin persisted until T20. They could still be observed at T40.

DISCUSSION

This new prototype of CLSM dedicated to *in vivo* skin exploration brought substantial improvements compared with previous systems (6–8). Sharper images of the epidermal keratinocytes could be recorded with the blue laser line (Figure 2a). This could be

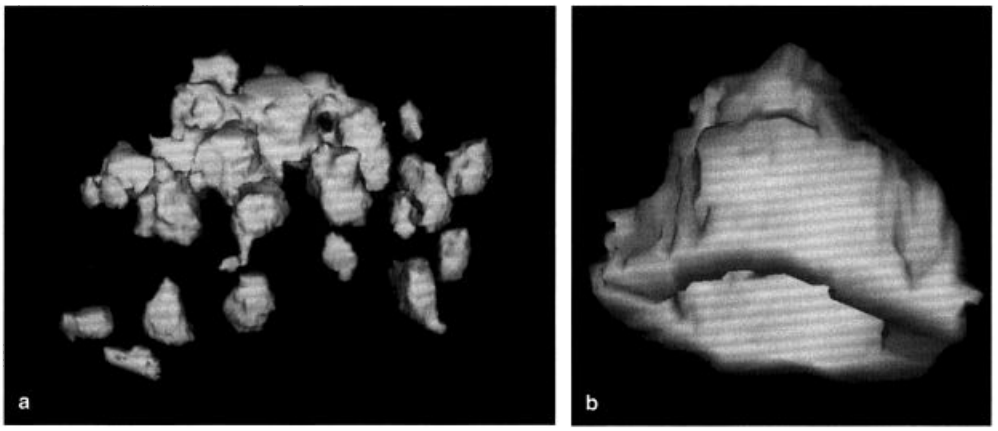

Figure 4. 3D reconstruction of the segmented bright features into the basal keratinocytes. (a) Overview of the bouquet overlaying a dermal papilla. (b) Detail of one feature zoomed and rotated in order to reveal the spherical imprint of the nucleus.

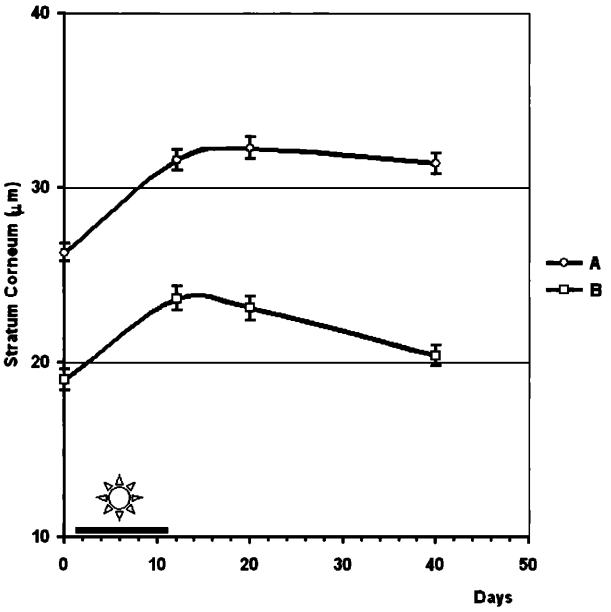

Figure 5. Sun exposure: evolution of the stratum corneum thickness following one-week sun exposure in subjects A and B.

anticipated since the Raleigh-limit formula predicts better resolution for shorter wavelengths. Nevertheless, other technical features could also be responsible for the unprecedented quality of the images. The use of a coherent light instead of white light can be considered, even though it has already been demonstrated that the laser source used generates side lobe effects (14) that may degrade resolution. This effect is not encountered with incoherent white light sources. The rather unusual high numerical aperture

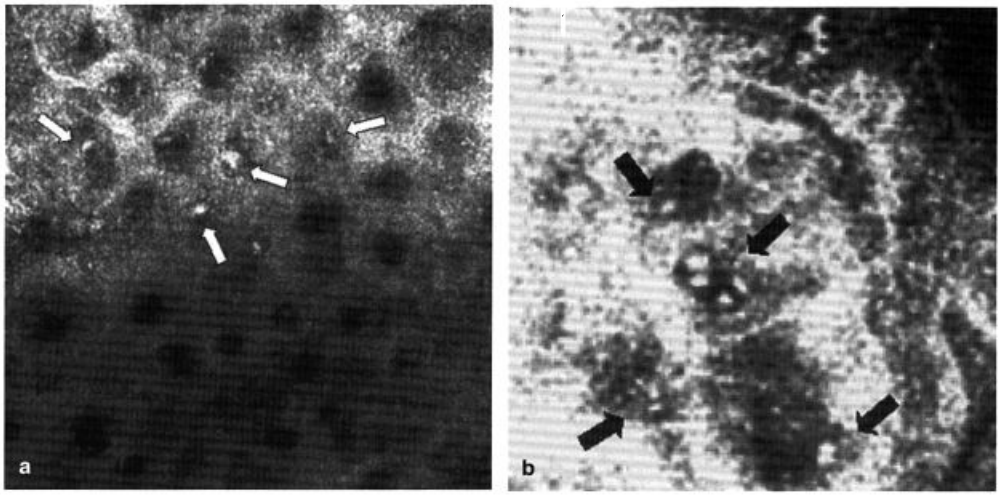

Figure 6. Sun exposure: condensation of the chromatin. (a) Presence of bright inclusions in numerous nuclei of granular and spinous keratinocytes; subject B, T20. Image size: 168 × 168 µm. (b) Zoomed image of four nuclei showing several bright inclusions in each; subject B, T12. Image size: 42 × 42 µm.

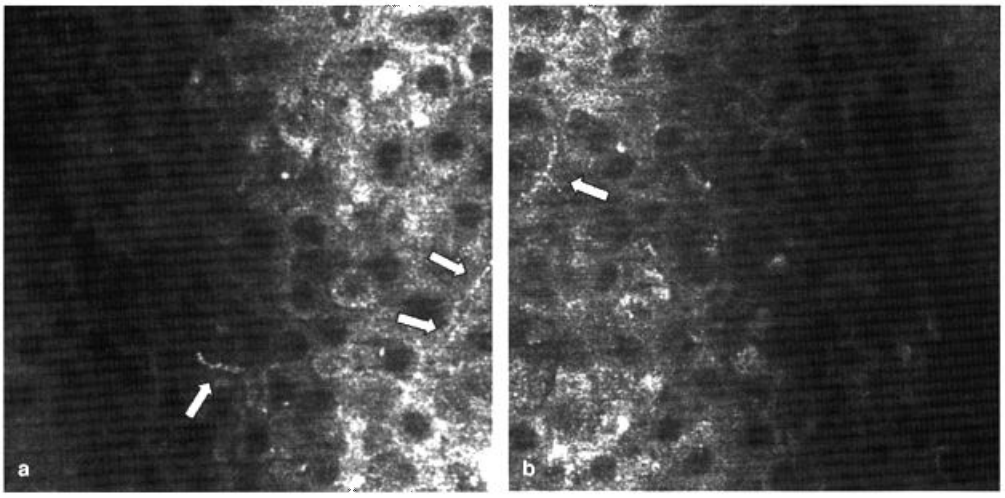

Figure 7. Sun exposure: migration of melanosomes. Two pictures showing the presence of bright spotted filaments in the intercellular spaces of the epidermal spinous layers. (a) Upper layers. (b) Lower layers. Subject B, T12. Image size: 168 × 168 μm.

of 1.30 for a ×40 objective lens certainly plays a role in increasing the axial and lateral resolution. Other lenses have been tested, in particular infinity-corrected objectives that introduced unexpected and unfortunate back reflections. Even though the laser power was limited to 2 mW at the objective lens, it provided a much larger light budget than the 1% of the light transmitted by the Nipkow disk of the TSM. There were also improvements made in the design of the contact stabilization device. By providing the axial displacement of the objective lens with a long-stroke piezoelectric translator with 0.1-μm precision, as opposed to moving the contact tip with a stepping motor of 1-μm step, a gain in precision was added to a gain in stability at the fixed skin surface. The

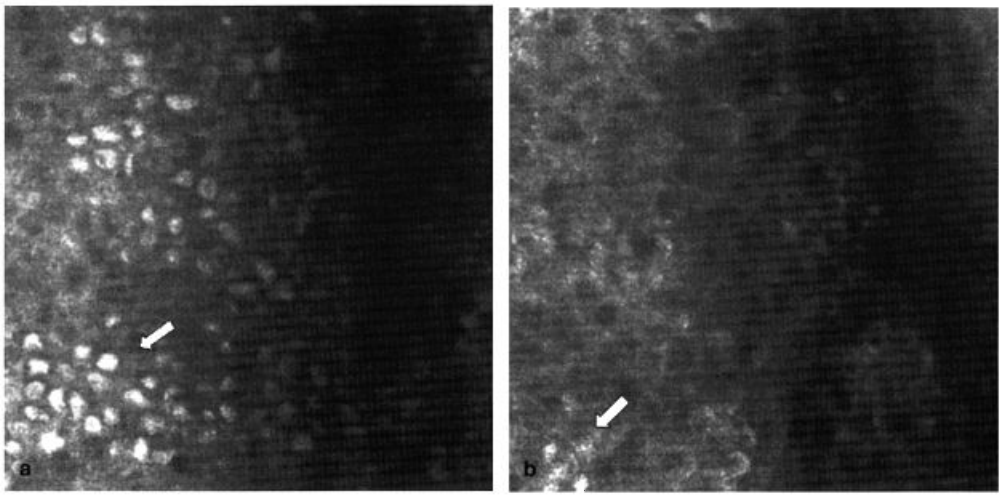

Figure 8. Sun exposure: the lack of melanosome caps. (a) Before exposure, basal cells exhibit bright melanosome clusters. (b) After exposure, bright caps are almost missing; a few are indicated by the white arrow. Subject B, T20. Image size: 168 × 168 μm.

resultant lateral stability was judged to be exceptional. Controlling the coarse approach of the confocal module to the skin surface with a motorized stage was found to be not only convenient but also very precise.

The images of the keratinocytes exhibited unexpected details (Figure 2a). The plasma membranes were clearly depicted; bright clusters and even granules in the cytoplasm could be observed. However, it is still impossible to unmistakably identify rare epidermal cell lines such as melanocytes and Langerhans cells.

The comparison of identical optical sections acquired with the three available wavelengths did not produce the expected results (15). If the blue line gave sharper images than the red one, the difference remained relatively modest. On the other hand, even though the red line penetrates deeper into the skin, imaging with this wavelength seemed to be limited by the very strong scattering properties of the dermal network. The gain in depth could be estimated to be only 20 μm. A good compromise was provided by the intermediate laser line in the green region (568 nm) that allowed exploration down to the papillary dermis. However, images of the reticular dermis (>150 μm in depth) could only be acquired with the red light. These images contain information not easily interpreted due to a lack of experience in the comprehension of images never before observed.

The blood flow in the capillaries could be readily seen with the green laser. By zooming in on an individual capillary, time-resolved displacement of individual leukocytes could be followed. Direct videotape recording of live images remains the best mode of storage (16) since it does not have the recording time limitations of digital storage.

It has been previously reported that melanin provides the contrast in the epidermal structures using *in vivo* confocal microscopy (7,8). Darker skin provides higher contrast. Thus, the bright bouquets and the crowns at the dermo-epidermal interface (Figure 2b) are never seen in a plaque of vitiligo. Rarely seen in skin phototype I, they are observed in only 60% of phototype II and always in darker skins. The best contrast is obtained in Negroid skin from which increased papillomatosis and its big dermal papillae lead to spectacular images at the dermo-epidermal junction.

The 3D reconstruction of the bright features from the basal cells (Figure 3a) allowed a definite association with the melanin caps (Figure 3b) covering the apical pole of the nucleus (17). Even though observed on vertical sections using a conventional transmission light microscope, the melanin can easily be identified as absorbing clusters without employing any specific staining (Figure 9). The specific location of the melanin cap has been previously interpreted as a protection of the basal nuclei against injury from the sun (18). Absorption of light by melanin has been largely reported in the literature (19–21). Melanin absorption coefficients have been calculated. They increase rapidly at shorter wavelengths and reach a maximum in the UV region (5). The role of the melanin cap has been explained as a hat covering and protecting the nucleus to avoid DNA damage by UV rays (18). In the scanning electron microscope, the melanin cap consists of a cluster of capsule-shaped melanosomes (Figure 10a). Melanosomes are lisosome-like organelles containing tightly packed melanin proteins enclosed in a plasma membrane (22). They have a diameter of 200 nm and a length of 800 nm (Figure 10b). Their size is close to the Raleigh limit of the confocal microscope. Consequently, they have the potential to generate an optical signal in terms of reflection and/or multiple scattering

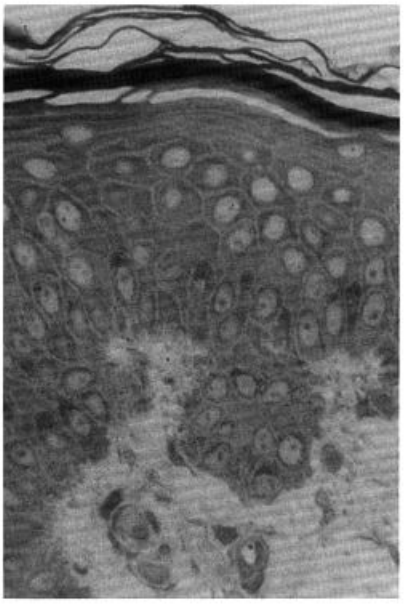

Figure 9. Semi-thin histological section of a Negroid skin sample exhibiting melanin clusters above the nucleus of basal cells. Courtesy of F. Fiat.

(23). The abrupt mismatch in the refractive index between the cytoplasm (~1.33) and the protein content of the melanosomes (~1.55) (24) is large enough to generate a strong reflection at the surface of the plasma membrane of the melanosome. Thus, melanosomes could act as myriads of nanomirrors reflecting sunbeams and protecting the nucleus against injury. This hypothesis suggests that the wavelength independent reflection process would be effective in the whole light spectrum and could contribute to the limiting of the penetration of light into the nucleus. The residual part penetrating into the melanosome would then be scattered and absorbed by the melanin. The residual protection by absorption is indeed much more efficient in the UV than in the visible part

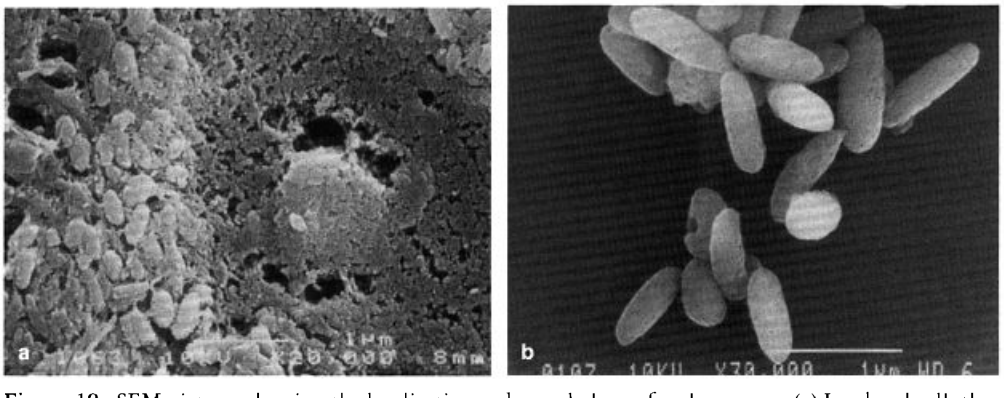

Figure 10. SEM pictures showing the localization and morphology of melanosomes. (a) In a basal cell, they form tightly packed clusters within the cytoplasm. (b) At a higher magnification, their shape and size can be evaluated. White bar = 1 μm. Courtesy of A. M. Minondo.

of the sun spectrum. It is inconceivable to limit the protection to absorption only. This would lead to a colossal storage of energy that would need to be dissipated by the cell. Such a process still remains unknown.

The effects of sun exposure on the physiology of the epidermis have largely been reported in the literature. The well-known hyperkeratosis (25,26) has been measured *in vivo* for the first time by confocal microscopy (Figure 5). This demonstrates the unique performance of this device in measuring noninvasively the thickness of the epidermal layers. Today, confocal microscopy remains the only technology providing rapid thickness measurements of the epidermal layers with a precision on the order of the micrometer. This avoids the need to perform painful biopsies on human volunteers. A 25% increase in stratum corneum thickness on each of the two subjects was recorded for a period of one month post-exposure. In this experiment, the epidermal hyperplasia of the epidermis *in vivo* could not be determined. The only explanation for this is that such a measurement needs a marker formed by the bright signal of the basal keratinocytes that was lacking after exposure.

Sun-exposed forearms led to unusual images through the confocal microscope. These unusual images were not observed before exposure and disappeared one month after exposure. These transient changes lasted for at least three weeks and consequently could not be attributed to a random phenomenon.

The bright inclusions in the nuclei of numerous granular and spinous keratinocytes (Figure 6) can be interpreted as local condensations of chromatin. This would generate an index mismatch and consequently would lead to high reflections at the interface. Condensation of the chromatin seems to be in accordance with the histologic description of sunburn cells (27–29).

Brightly spotted filaments in the intercellular spaces between keratinocytes (Figure 7) could correspond to aligned melanosomes migrating towards the surface via the dendrites of melanocytes (20,22). It has been stated that in normal conditions the dendritic epidermal cell lines could not be clearly identified with the *in vivo* confocal microscope. This experiment has demonstrated, to the contrary, that only the dendrites but not the body of the melanocytes can be observed in exposed skin.

The most striking transient observation turned out to be the total lack of melanosome caps in basal keratinocytes (Figure 8b) for a period of three weeks following sun exposure. A possible first explanation could be that photodegradation (30) or redox mechanisms (31) liberate the melanin contents of the melanosomes. Their geometry would thus not permit any further optical signal except for a diffuse absorption that is responsible for the tanned aspect of the upper layers. A second explanation could be related to the slow formation of melanosomes by the melanocytes, limiting both their increased migration towards the skin surface and the renewal of the reservoir in the basal keratinocytes (19–20).

CONCLUSION

The new phototype of CLSM dedicated to the exploration of human skin *in vivo* provides major improvements when compared to previous systems. Sharper images were recorded with the blue laser line (488 nm), while the red line (647 nm) provided better pen-

etration into the dermis. The observation of unexpected details in epidermal cells, real-time tracking of blood cells and fast 3D reconstruction of the skin *in vivo,* point to promising paradigms in skin research. These additional performances allowed for a definite explanation of the strong reflection of the basal keratinocytes: the melanosome caps acted as myriads of nanomirrors.

A cascade of physiological events following sun exposure was recorded: a 25% increase in the stratum corneum thickness, a condensation of the chromatin in numerous keratinocytes, the suspected migration of the melanosomes via the dendrites of melanocytes, as well as the lack of melanosome caps in the basal keratinocytes. All of these events disappeared one month after exposure.

It is now possible to observe that which was impossible before. *In vivo* confocal microscopy opens up new challenges in the understanding of skin optics and melanogenesis.

ACKNOWLEDGMENT

The authors wish to thank Daniel Good for his expert assistance in the correction of the manuscript.

REFERENCES

(1) M. J. Van Gemert, S. L. Jacques, H. J. Sterenborg, and W. Star, Skin optics, *IEEE Trans. Biomed. Eng.,* **36,** 1146–1154 (1989).
(2) J. B. Dawson, D. J. Barker, D. Ellis, E. Grassam, J. A. Cotterill, G. W. Fisher, and J. W. Feather, A theoretical and experimental study of light absorption and scattering by *in vivo* skin, *Phys. Med. Biol.,* **25,** 695–710 (1980).
(3) P. H. Anderson and P. Bjerring, Spectral reflectance of human skin *in vivo, Photodermatol. Photoimmunol. Photomed.,* 7, 5–12 (1990).
(4) D. Contini, G. Zaccanti, F. Martelli, and A. Sassaroli, Models for photon migration and optical properties of biological tissues, *Phys. Scr., T,* **72,** 76–82 (1997).
(5) S. L. Jacques, Skin optics, *Oregon Medical Laser Center News* (January 1998).
(6) K. C. New, W. M. Petroll, A. Boyde, L. Martin, P. Corcuff, J. L. Lévêque, M. A. Lemp, H. D. Cavanagh, and J. V. Jester, *In vivo* imaging of human teeth and skin using real-time confocal microscopy, *Scanning,* **13,** 369–372 (1991).
(7) P. Corcuff, C. Bertrand, and J. L. Lévêque, Morphometry of human epidermis *in vivo* by real-time confocal microscopy, *Arch. Dermatol. Res.,* **285,** 475–481 (1993).
(8) M. Rajadhyaksha, M. Grossman, D. Esterowitz, R. H. Webb, and R. R. Anderson, *In vivo* confocal scanning laser microscopy of human skin: Melanin provides strong contrast, *J. Invest. Dermatol.,* **104,** 946–952 (1995).
(9) P. Corcuff, G. Gonnord, G. E. Piérard, and J. L. Lévêque, *In vivo* confocal microscopy of human skin: A new design for cosmetology and dermatology, *Scanning,* **18,** 351–355 (1996).
(10) B. R. Masters, G. Gonnord, and P. Corcuff, Three-dimensional microscopic biopsy of *in vivo* human skin: A new technique based on a flexible confocal microscope, *J. Microsc.,* **185,** 329–338 (1997).
(11) S. Mallat, A theory for multiresolution signal decomposition: The wavelet representation, *IEEE Trans. Pattern. Anal. Mach. Intell.,* **11,** 674–693 (1989).
(12) S. W. Zucker, Region growing: Childhood and adolescence, *Comput. Graphics Image Process.,* **5,** 382–399 (1976).
(13) T. B. Fitzpatrick, The validity and practicality of sun reactive skin type I through IV (editorial), *Arch. Dermatol.,* **124,** 869–871 (1988).
(14) D. T. Fewer, S. J. Hewlett, and E. M. McCabe, Laser sources in direct-view-scanning, tandem-scanning, or Nipkow-disk-scanning confocal microscopy, *Applied Optics,* 37, 380–385 (1998).

(15) P. Corcuff, C. Hadjur, C. Chaussepied, and R. Toledo-Crow, Confocal laser microscopy of the *in vivo* human skin revisited, *SPIE Proc.,* **3605,** 73–81 (1999).
(16) C. Bertrand and P. Corcuff, *In vivo* spatio-temporal visualization of the human skin by real-time confocal microscopy, *Scanning,* **16,** 150–154 (1994).
(17) M. Rajadhyaksha, S. Gonzàlez, J. M. Zavislan, R. R. Anderson, and R. H. Webb, *In vivo* confocal laser scanning microscopy of human skin. II: Advances in instrumentation and comparison with histology, *J. Invest. Dermatol.,* **113,** 293–303 (1999).
(18) N. Kobayashi, A. Nakagawa, T. Muramatsu, Y. Yamashina, T. Shirai, M. W. Hashimoto, Y. Ishigaki, T. Ohnishi, and T. Mori, Supranuclear melanin caps reduce ultraviolet induced DNA photoproducts in human epidermis, *J. Invest. Dermatol.,* **110,** 806–810 (1998).
(19) T. B. Fitzpatrick, M. Miyamoto and K. Ishikawa, The evolution of concepts of melanin biology, *Arch. Dermatol.,* **96,** 305–323 (1965).
(20) A. J. Thody, Epidermal melanocytes: Their regulation and role in skin pigmentation, *Eur. J. Dermatol.,* **5,** 558–565 (1995).
(21) M. R. Chedekel, "Photophysics and Photochemistry," in *Melanin: Its Role in Human Photoprotection,* L. Zeise, M. R. Chedekel, and T. B. Fitzpatrick, Eds. (Valdenmar Publishing Co, Overland Park, KS, 1995), pp. 11–22.
(22) O. Yamamoto and J. Bhawan, Three modes of melanosomes transfer in Caucasian facial skin: Hypothesis based on an ultrastructural study, *Pigment Cell Res.,* **7,** 156–169 (1994).
(23) R. R. Anderson and J. A. Parrish, The optics of human skin, *J. Invest. Dermatol.,* 77, 13–19 (1981).
(24) R. J. Scheuplein, A survey of some fundamental aspects of the absorption and reflection of light by tissue, *J. Soc. Cosmet. Chem.,* **15,** 111–122 (1964).
(25) A. D. Pearse, S. A. Gaskell, and R. Marks, Epidermal changes in human skin following irradiation with either UVA or UVB, *J. Invest. Dermatol.,* **88,** 83–87 (1987).
(26) R. M. Lavker, G. F. Gerberick, D. Veres, C. J. Irwin, and K. H. Kaidbey, Cumulative effects from repeated exposures to suberythemal doses of UVB and UVA in human skin, *J. Am. Acad. Dermatol.,* **32,** 53–62 (1995).
(27) A. R. Young, The sunburn cell, *Photo-Dermatol.,* 4, 127–134 (1987).
(28) R. Linse and G. Richard, Histology of UV-induced epidermis reactions. 1. A contribution to the differentiation of sunburn cells, *Dermatologishe Monatsschrift,* **176,** 345–348 (1990).
(29) C. Bayerl, S. Taake, I. Moll, and E. G. Jung, Characterization of sunburn cells after exposure to ultraviolet light, *Photodermatol. Photoimmunol. Photomed.,* **11,** 149–154 (1995).
(30) N. Kollias, "The Spectroscopy of Human Melanin Pigmentation," in *Melanin: Its Role in Human Photoprotection,* L. Zeise, M. R. Chedekel, and T. B. Fitzpatrick, Eds. (Valdenmar Publishing Co, Overland Park, KS, 1995), pp. 31–38.
(31) J. Borovansky, P. Hach, K. Smetana Jr., M. Elleder, and I. Matous-Malbohan, Attempts to induce melanosome degradation *in vivo, Folia Biologica* (*Praha*), **45,** 47–52 (1999).